

CrossMark
click for updatesCite this: *RSC Adv.*, 2016, 6, 8198

Evaluation of the characteristics of non-oxidative biodiesels: a FAME composition, thermogravimetric and IR analysis

I. Shancita,* H. H. Masjuki, M. A. Kalam,* S. S. Reham, A. M. Ruhul and I. M. Monirul

This experiment evaluates the effects of non-oxidative biodiesel (low oxygen content biodiesels) characteristics and their engine performances. Biodiesels produced from different feedstocks typically contains 10% to 15% oxygen by weight, which enhances the combustion quality and reduces the emissions of hydrocarbons (HCs) and carbon monoxide (CO). However, it produces a higher amount of nitrogen oxides (NO_x) due to an increasing number of combustion products, resulting in a higher cylinder temperature. In addition, lean air–fuel mixtures can contribute to higher NO_x emissions because biodiesel is more oxygenated than diesel. In this study, biodiesels produced from different feedstocks by a transesterification process were used to reduce the oxygen content by dipping an iron bar in the biodiesels, which absorbs oxygen and gets oxidized. Then, the oil characteristics, such as the percentage of saturated and unsaturated fatty acids, thermal degradation, stability and existing functional groups, were analyzed using fatty acid methyl ester (FAME) composition analysis, thermogravimetric analysis (TGA), differential scanning calorimetry (DSC) and Fourier transform infrared (FT-IR) spectroscopy analysis of neat biodiesel and non-oxidative biodiesel. Herein, *Pongamia* and *Moringa* biodiesels, containing normal and reduced weight percentages of oxygen, were evaluated to improve the quality and stability of biodiesels used in the diesel engine, which will also reduce the NO_x emissions. Non-oxidative biodiesels had some positive effect on their properties, which can further reduce the NO_x emissions. Herein, non-oxidative *Pongamia* and *Moringa* had quite similar characteristics and the former was observed to perform better in the reduction of NO_x and other emissions as well.

Received 13th November 2015
Accepted 23rd December 2015

DOI: 10.1039/c5ra23963j

www.rsc.org/advances

1. Introduction

Nowadays, biodiesel is one of the most suitable alternative energy providers for industrial, transportation and domestic consumption as they are a renewable, eco-friendly, readily available, biodegradable and non-toxic resource. Biodiesel can be used in its pure form or mixed with diesel in any volume percentage; moreover, it is feasible to be used in the diesel engine without any modification of the engine.^{1,2} Although biodiesel emits almost zero sulfur oxides, and has 14.2% less HC, 26.8% less PM and 9.8% less CO_2 emissions than diesel fuel, its negative impact on NO_x emissions raises several questions regarding environmental pollution.^{3,4} Biodiesel is typically produced by a transesterification reaction, in which triglycerides of vegetable oils or animal fats are reacted with short chain alcohol, such as methanol or ethanol, to produce the corresponding mono-alkyl esters and glycerin. Biodiesel is mainly a mixture of different fatty acid methyl esters (FAME) containing

long chain, highly concentrated mono and poly unsaturated compounds.^{5,6}

Typically, neat biodiesel consists of 11–15 wt% oxygen, which is the main cause for the improvement of combustion efficiency of biodiesel. On the other hand, it degrades the biodiesel stability and also makes it less efficient than fossil fuel and cannot be used in airplanes. Moreover, it increases the emissions of NO_x although it decreases HC and CO emissions. This results in products of combustion, triggered by the higher oxygen content, which increases the temperature of the combustion chamber, thus improving combustion efficiency and consequently promoting NO_x formation.^{4,7,8} In this study, the oxygen percentage in biodiesel, termed as a non-oxidative biodiesel, is decreased in an optimum amount with an aim to reduce NO_x emissions. These reformed biodiesels were obtained from low temperature oxidation process in an iron–oxygen bath. The iron bar absorbed the oxygen molecule from the biodiesels. These biodiesels were characterized by FAME composition, TGA, DSC and FT-IR analysis.

Thermal degradation, FAME composition and IR characteristics of biodiesel are important quality assessment sources for biodiesel to be commercially used in a diesel engine. Thermal characteristics give the information about thermal stability and

Centre for Energy Sciences, Department of Mechanical Engineering, Faculty of Engineering, University of Malaya, 50603 Kuala Lumpur, Malaysia. E-mail: shancita@um.edu.my; kalam@um.edu.my; Fax: +603 79675317; Tel: +603 79674448

volatility of a biodiesel by measuring heat capacity, enthalpy, activation energy and melting point.^{2,7} Thermogravimetric analysis (TGA) is considered as a thermoanalytical technique, which measures the change in mass of a substance as a function of increasing temperature at a constant rate. The loss in mass of a substance with the increase in temperature may be caused by decomposition, oxidation or vaporization. A derivative of the weight loss curve is normally used to obtain the decomposition or vaporization temperature for pure as well as mixed compounds. On the other hand, differential scanning calorimetry (DSC) is used together with TGA and also is a thermoanalytical technique. It typically measures the energy required for the temperature increase of the substance studied. DSC curves provide important information about enthalpy of boiling, melting, oxidation and decomposition. An endothermic weight loss is accounted for endothermic decomposition or boiling and exothermic weight loss is attributed for exothermic oxidation or decomposition of the substance.^{9,10} Many studies used thermogravimetric analysis for the measurement of stability and production rate of biodiesels. Jain *et al.*¹¹ reported the effect of antioxidants on the thermal degradation of *Jatropha curcas* biodiesel. By varying the concentration and type of antioxidants, various thermodynamic properties of biodiesel, such as activation energy (E_a), onset temperature (T_{on}) and offset temperature (T_{off}), were measured by TGA analysis. This study helped to improve the thermal stability of the biodiesel thermal by selecting the suitable additives in an engine fuel. On the other hand, Vega-Lizama *et al.*¹ conducted their research on the measurement of thermal degradation degree of soy biodiesel using the residual mass obtained from the decomposition curve. The obtained results showed that TGA analysis is an efficient method to determine the oxidation degree of biodiesel without knowing the biodiesel oxidation process. Moreover, Niu *et al.*² studied the thermal degradation of different biodiesels produced from different feedstocks through transesterification process by TGA analysis. Moreover, the combustion characteristics of palm and rapeseed biodiesels by thermogravimetric analysis was studied by Yuan *et al.* in the furnace of a thermogravimetry-differential scanning calorimetry (TGA-DSC) thermal analyzer instead of a diesel engine.⁷ This study was focused on comparing the suitability of non-oxidative biodiesels with neat biodiesels and diesel, which will affect the engine performance and exhaust emissions characteristics.

2. Materials and methods

2.1 Materials

Crude *Moringa* and *Pongamia* oils were collected from India. The characteristics of these crude oils are listed in Table 3. The diesel fuel (B0) was purchased from PETRONAS. Other materials, reagents, and chemicals, such as methanol, H_2SO_4 , KOH, and Na_2SO_4 , were obtained from LGC Scientific Sdn. Bhd. (Malaysia).

2.2 Production of *Pongamia* and *Moringa* biodiesels

The production of *Pongamia* and *Moringa* biodiesels from their corresponding crude oils was performed in the energy

laboratory of the University of Malaya. A 1 L batch reactor equipped with a flux condenser, magnetic stirrer, thermometer, and sampling outlet were used to produce biodiesels. Crude *Moringa* oil was transesterified to produce biodiesel from it as the acid value was less than 4 mg KOH per g. On the other hand, for *Pongamia* biodiesel production, to reduce the high acid value of feedstocks, a two-step process, involving esterification and transesterification, was performed. First, *Moringa* oil was reacted with 25% (v/v oil) methanol (6 : 1 molar ratio) and 1% (w/w oil) potassium hydroxide (KOH) and maintained at 60 °C and 600 rpm for 2 h. After the reaction, the mixture was deposited in a separation funnel for 12 h to separate glycerol from the produced biodiesel. The lower layer containing glycerol and impurities was drained. In the post-treatment process, the methyl ester formed from the previous process was washed with hot distilled water at 60 °C to remove glycerol and impurities. The upper layer was poured into a control rotary evaporator (IKA) to remove water and excess methanol from methyl ester, whereas the lower layer was drained. Methyl ester was dried using Na_2SO_4 . The produced biodiesel was filtered using a qualitative filter paper to obtain the final product. For the *Pongamia* oil, in the esterification process, the molar ratio of methanol was maintained at 12 : 1 (50% v/v oil), and 1% (v/v oil) sulfuric acid (H_2SO_4) was added to the pre-heated oils at 60 °C and 600 rpm for 3 h in a glass reactor to refine the crude oils. After reaction completion, the product was transferred to a separation funnel, in which the esterified oil (lower layer) was separated from the upper layer. The upper layer included excess alcohol, sulfuric acid, and impurities. The lower layer was then loaded into a control rotary evaporator (IKA) and heated at 60 °C under vacuum conditions for 1 h to remove methanol and water from the esterified oil. Then, during transesterification, the esterified oils were reacted with 25% (v/v oil) methanol and 1% (m/m oil) potassium hydroxide (KOH) and maintained at 60 °C and 600 rpm for 2 h. After reaction completion, the produced biodiesels were deposited in a separation funnel for 12 h to separate glycerol from the biodiesels. The upper layer was washed three times with hot distilled water. The formed methyl ester was poured into a control rotary evaporator (IKA) to remove water and excess methanol and then dried using Na_2SO_4 . The lower layer containing impurities and glycerol was drained. The produced methyl ester was filtered with a qualitative filter paper to obtain the final products as biodiesel.

2.3 Oxygen reducing process from biodiesels

The oxygen reducing process was conducted using a commercial grade iron bar of length 3 cm, width 1.5 cm and thickness 0.3 cm, which was dipped in the produced biodiesel. The iron bar was dipped in 10–20 mL biodiesels at 60 °C and 100 rpm after cleaning. All the biodiesels with iron bars were kept in airtight glass bottle at room temperature for 6 weeks. All the iron bars were weighted before and after the test period by a Scaltec SBA 31 (0.0001 g resolution). A change of weight of iron bars was observed for the 1.04% and 0.7% *Pongamia* and *Moringa* biodiesels, respectively. The iron bars were oxidized by reacting with oxygen from the biodiesels, which was the main

cause for reduced oxygen weight percentage in non-oxidative biodiesels than neat biodiesels.

2.4 Iron oxidation and elemental composition

The oxidation of iron bars due to the dipping in biodiesels was observed using a SEM (scanning electron microscope) model Hitachi TM3030 at 150 \times magnification with an acceleration voltage of the microscope of 5 kV while operating. Elemental composition of normal and oxidized iron bars has been analyzed by a Bruker Quantax 70 EDX (energy dispersive system) at 150 \times magnification attached with a microscope. Each bar was scanned at three different spots and their average result is reported in this article.

2.5 Fatty acid methyl ester (FAME) composition

The fatty acid methyl ester composition of neat and non-oxidative *Pongamia* and *Moringa* biodiesels was measured using gas chromatography (GC) analysis in an Agilent 7890A model equipped with a flame ionization detector with a HP-INNOWax column (30 m \times 0.25 mm, 0.25 μ m of thickness). The flow rate of carrier gas helium was 3.5 mL min⁻¹. The oven temperature was maintained at 50 $^{\circ}$ C for 5 min initially and then programmed to increase at a rate of 20 $^{\circ}$ C min⁻¹ to 210 $^{\circ}$ C and maintained for 18 min. Then, another increase was made to 230 $^{\circ}$ C at a rate of 20 $^{\circ}$ C min⁻¹, which was maintained for 13 min. Both the injector and detector temperature was maintained at 250 $^{\circ}$ C. A sample was injected at a split ratio of 50 : 1 of 0.3 μ L volume.

2.6 Property analysis of neat and non-oxidative biodiesels

Biodiesels can be characterized by several important physico-chemical properties that determine the quality and suitability of the biodiesels in order to be used in the unmodified diesel engine as a blend with diesel or in a pure form. In this study, some key characterization properties of neat and non-oxidative coconut, *Pongamia* and *Moringa* biodiesels are measured and compared, which include kinematic viscosity, density, calorific value, cetane number, oxidation stability and flash point. These physicochemical properties were measured according to the international standard specifications of ASTM D6751 or EN14214 and then compared between neat and non-oxidative biodiesels and also with conventional diesel.

2.7 Thermogravimetric (TGA) analysis

The TGA analysis test of neat, non-oxidative biodiesels and diesel was performed using a TGA Q500 V20.13 Build 39 thermal analyzer at a constant heating rate of 50 $^{\circ}$ C min⁻¹ under a nitrogen atmosphere at a flow rate of 40 mL min⁻¹. About 10–20 mg of samples was used in a 40 μ L platinum pan at temperature interval from 4.0 $^{\circ}$ C to 950 $^{\circ}$ C.

2.8 Differential scanning calorimetry (DSC) analysis

The DSC analysis test for neat, non-oxidative biodiesels and diesel was performed using an instrument named DSC Q200 V24.11 Build 124 DSC analytical module in a standard cell under inert (nitrogen) atmosphere with gas flow rate of 50 mL min⁻¹

and at a 10 $^{\circ}$ C min⁻¹ heating rate to 130 $^{\circ}$ C to heat the samples. DSC cell was loaded with one sample and one reference pan. About 10 mg of sample was placed in a sealed aluminum pan and one identical empty pan was set as a reference to perform the test. For heating scans, samples were cooled rapidly and held isothermally for 2 min at -60 $^{\circ}$ C and then heated to 130 $^{\circ}$ C and then the samples were held isothermally for 2 min at 130 $^{\circ}$ C, then cooled to -80 $^{\circ}$ C for cooling scans.

2.9 Fourier transform infrared (FTIR) spectroscopy analysis

The FTIR spectroscopy analysis of neat, non-oxidative biodiesels and diesel was done in a Perkin Elmer biodiesel FAME analyzer connected with an MIR TGS detector. The range of spectrum was 4000–450 cm⁻¹ and the resolution and scans were 4 cm⁻¹ and 16 scans, respectively. This spectrum was processed by e-spectrum software.

3. Results and discussions

3.1 Oxidation of iron bars to reduce the oxygen content of biodiesels

Fig. 1(a)–(c) present the SEM images of normal, oxidized iron bars from *Pongamia* and *Moringa* biodiesel, respectively. From the SEM images, we can observe the change in the iron bars from normal to oxidized mode due to reacting with oxygen in biodiesels, which in turns confirmed that the iron bars were oxidized. Moreover, it can be comprehended from the image that the iron bar from *Pongamia* biodiesel was more oxidized than the iron bar from *Moringa* biodiesel. As a result, there was higher reduction of oxygen content from *Pongamia* biodiesel than of *Moringa*. As the biodiesels were kept in an airtight opaque bottle, they were examined before and after the oxygen reduction process.

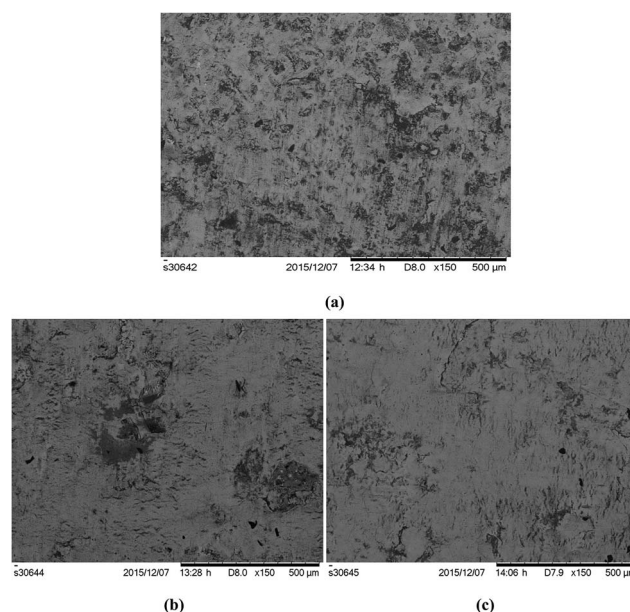


Fig. 1 SEM images of (a) normal iron, (b) oxidized iron (*Pongamia*) and (c) oxidized iron (*Moringa*).

3.1.1 Elemental composition analysis of normal and oxidized iron bars. The elemental composition of normal and oxidized iron bars was analyzed to observe the main components of the bars before and after the oxidation process. Results were obtained from three different spots and the atomic percentage of elements are presented in Fig. 2. The elements presented in the bars were oxygen, iron and carbon. From the Fig. 2(a)–(c), it can be seen that the atomic percentage of oxygen of normal and oxidized iron bars was different and the iron bar from *Pongamia* biodiesel had higher oxygen molecule content than the iron bar from *Moringa* biodiesel. However, the elemental composition also confirmed the oxidation of iron bars due to the reaction with oxygen from the biodiesels as the oxygen percentage increases from normal to oxidized mode and therefore, higher oxygen reduction from *Pongamia* biodiesel is obtained.

3.2 FAME composition of neat and non-oxidative biodiesels

In Table 1, the FAME composition of neat and non-oxidative *Pongamia* and *Moringa* biodiesels are presented. The saturated and unsaturated fatty acid composition of both the neat and non-oxidative biodiesels is compared to determine the most suitable one for better performance.

The monounsaturated fatty acid was same for both the neat and non-oxidative *Pongamia* biodiesels, whereas it increased for *Moringa* biodiesel from the neat to non-oxidative mode. These biodiesels consisted mainly of oleic acid C 18 : 1 (50.9%) and (50.8%) and eicosenoic acid C 20 : 1 (1.2%) and (1.3%) for neat and non-oxidative *Pongamia* biodiesel. Moreover, the *Moringa*

biodiesel consisted of oleic acid C 18 : 1 and eicosenoic acid C 20 : 1 as (25.2% and 32.1%) and (0.3% and 0.2%) for neat and non-oxidative mode, respectively. Other unsaturation percentage was completed by polyunsaturated fatty acid, which was due to the presence of linoleic C 18 : 2 and linolenic acid C 18 : 3. For both *Pongamia* and *Moringa* biodiesel, the percentage of linoleic (18.2% to 17.0% and 52.1% to 44.1%) and linolenic (4.0% to 3.6% and 6.0% to 4.6%) acid was decreased from neat to non-oxidative mode, which resulted in the total decrease in poly-unsaturation of both biodiesels from neat to non-oxidative mode. High mono-unsaturated fatty acid resulted in high oxidation stability of *Pongamia* biodiesel, which was also confirmed from the test. Moreover, low amount of polyunsaturated fatty acid develops higher cetane number and also produces lower emissions of NO_x .^{12–15} On the other hand, the saturated fatty acid composition was same for *Moringa* but increases for *Pongamia* biodiesel from neat to non-oxidative mode. The highest saturated fatty acid was palmitic C 16 : 0 (9.7% to 10.2% and 10.8% to 10.9%), followed by stearic C 18 : 0 (6.8% to 6.9% and 4.4% to 4.0%), behenic C 22 : 0 (5.6% to 5.6% and 0.4% to 0.4%) and arachidic C 20 : 0 (1.6% to 1.7% and 0.4% to 0.4%) for *Pongamia* and *Moringa* biodiesel from neat to non-oxidative mode. Biodiesels containing highly saturated fatty acids have low quality cold flow properties and also they have high melting points.^{12,14} In this study, both the biodiesels had low amount of saturated fatty acids and high amount of monounsaturated fatty acid with a higher value in *Pongamia* biodiesel for both neat and non-oxidative mode. These results are comparable with the previous literatures.^{16–22}

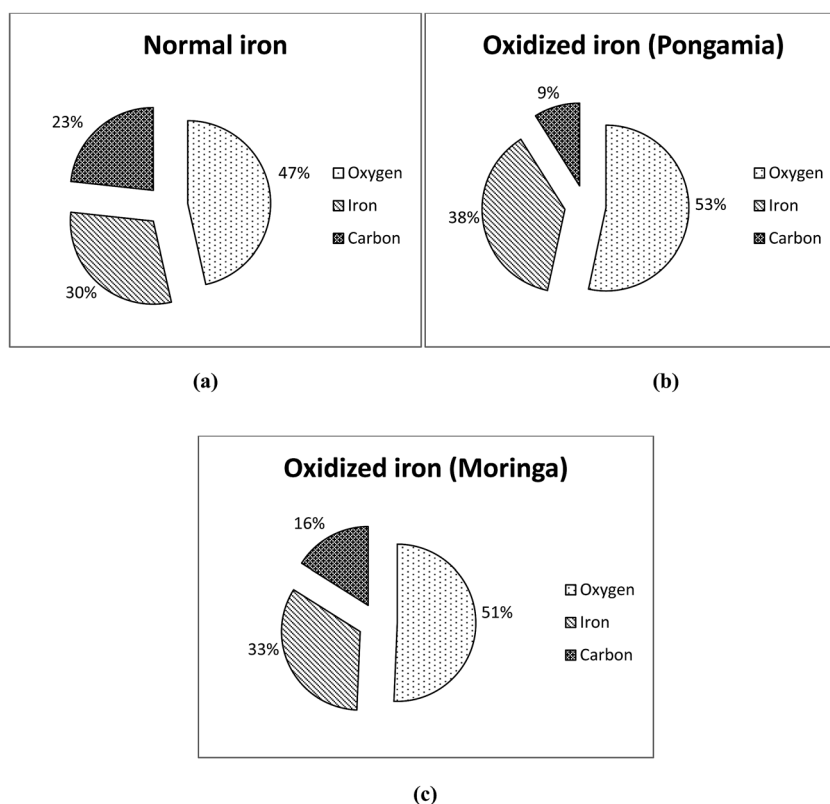


Fig. 2 Elemental composition of (a) normal iron, (b) oxidized iron (*Pongamia*) and (c) oxidized iron (*Moringa*).

Table 1 Fatty acid composition of neat and non-oxidative *Pongamia* and *Moringa* biodiesels

FAME	Structure	Molecular weight	Formula	Neat biodiesels		Non-oxidative biodiesels	
				<i>Pongamia</i> (wt%)	<i>Moringa</i> (wt%)	<i>Pongamia</i> (wt%)	<i>Moringa</i> (wt%)
Methyl hexanoate	6 : 0	130.18	CH ₃ (CH ₂) ₄ COOCH ₃	—	<0.1	<0.1	<0.1
Methyl octanoate	8 : 0	158.24	CH ₃ (CH ₂) ₆ COOCH ₃	<0.1	<0.1	<0.1	<0.1
Methyl decanoate	10 : 0	186.29	CH ₃ (CH ₂) ₈ COOCH ₃	<0.1	<0.1	<0.1	<0.1
Methyl laurate	12 : 0	214.34	CH ₃ (CH ₂) ₁₀ COOCH ₃	<0.1	<0.1	0.1	<0.1
Methyl myristate	14 : 0	242.39	CH ₃ (CH ₂) ₁₂ COOCH ₃	<0.1	<0.1	0.1	0.1
Methyl palmitate	16 : 0	270.45	CH ₃ (CH ₂) ₁₄ COOCH ₃	9.7	10.8	10.2	10.9
Methyl palmitoleate	16 : 1	268.43	CH ₃ (CH ₂) ₅ CH=CH(CH ₂) ₇ COOCH ₃	<0.1	0.1	<0.1	0.2
Methyl heptadecanoate	17 : 0	284.48	CH ₃ (CH ₂) ₁₅ COOCH ₃	—	—	0.1	0.1
Methyl(Z)-heptadec-10-enoate	17 : 1	282.46	CH ₃ (CH ₂) ₅ CH=CH(CH ₂) ₈ COOCH ₃	—	—	<0.1	0.1
Methyl stearate	18 : 0	298.50	CH ₃ (CH ₂) ₁₆ COOCH ₃	6.8	4.4	6.9	4.0
Methyl oleate	18 : 1	296.49	CH ₃ (CH ₂) ₇ CH=CH(CH ₂) ₇ COOCH ₃	50.9	25.2	50.8	32.1
Methyl linoleate	18 : 2	294.47	CH ₃ (CH ₂) ₄ CH=CHCH ₂ CH=CH(CH ₂) ₇ COOCH ₃	18.2	52.1	17.0	44.1
Methyl linolenate	18 : 3	292.46	CH ₃ CH ₂ CH=CHCH ₂ CH=CHCH ₂ CH=CH(CH ₂) ₄ COOCH ₃	4.0	6.0	3.6	4.6
Methyl archidate	20 : 0	326.56	CH ₃ (CH ₂) ₁₈ COOCH ₃	1.6	0.4	1.7	0.4
Methyl eicosenoate	20 : 1	324.54	CH ₃ (CH ₂) ₇ CH=CH(CH ₂) ₉ COOCH ₃	1.2	0.3	1.3	0.2
Methyl behenate	22 : 0	354.61	CH ₃ (CH ₂) ₂₀ COOH	5.6	0.4	5.6	0.4
Methyl erucate	22 : 1	352.59	CH ₃ (CH ₂) ₇ CH=CH(CH ₂) ₁₁ COOH	—	0.2	—	—
Methyl lignocerate	24 : 0	382.66	CH ₃ (CH ₂) ₂₂ COOH	1.6	0.1	1.6	0.2
Other				0.4	—	1.0	2.6
	Saturation			25.3	16.1	26.3	16.1
	Mono-unsaturated			52.1	25.8	52.1	32.6
	Poly-unsaturated			22.2	58.1	20.6	48.7
	Total			99.6	100	99	97.4

3.3 Elemental composition of neat and non-oxidative biodiesels

Table 2 presents the elemental composition of neat and non-oxidative *Pongamia* and *Moringa* biodiesels. In general, biodiesel contains carbon, hydrogen and oxygen, whereas diesel contains only carbon and hydrogen. Although high oxygen content in biodiesel helps to reduce CO and HC emissions by the complete combustion process that influences the oxidation of unburned hydrocarbons, which in turns increase the NO_x emissions by increasing the combustion chamber temperature. On the other hand, for reducing the NO_x emissions produced from biodiesels, non-oxidative *Pongamia* and *Moringa* biodiesels containing optimum amount of oxygen helps to reduce the CO and HC emissions as well as decreases the NO_x

emissions unlike the typical biodiesels. From the table, it can be seen that neat *Pongamia* biodiesel contains higher oxygen and hydrogen content, whereas had lower carbon content than that of the *Moringa* biodiesel. Therefore, *Pongamia* biodiesel had more complete combustion characteristics, which also increase the NO_x emissions. The reduction of oxygen weight percentage observed was 1.9% and 1.4% for *Pongamia* and *Moringa* biodiesels, respectively. Moreover, the carbon percentage increases for both biodiesels from neat to non-oxidative mode, which can be due to the iron bar that had lower carbon percentage from normal to oxidized mode. From the table, it can be concluded that non-oxidative *Moringa* had the lowest oxygen content hence it more suitable for NO_x reduction, although the reduction percentage was higher for *Pongamia* biodiesel.

Table 2 Elemental composition of neat and non-oxidative *Pongamia* and *Moringa* biodiesels

Wt%	Test method	Neat biodiesels		Non-oxidative biodiesels		Diesel
		<i>Pongamia</i>	<i>Moringa</i>	<i>Pongamia</i>	<i>Moringa</i>	
Carbon (C)	ASTM D5291	74.0	75.8	76.1	77.1	85.2
Hydrogen (H)	ASTM D5291	12.4	12.3	12.2	12.4	14.8
Oxygen (O)	ASTM D5291	13.6	11.9	11.7	10.5	0
C/H	—	5.97	6.16	6.24	6.22	5.76
Empirical formula	—	C _{6.17} H _{12.3} O _{0.85}	C _{6.32} H _{12.2} O _{0.74}	C _{6.34} H _{12.1} O _{0.73}	C _{6.43} H _{12.3} O _{0.66}	C _{7.1} H _{14.68}

Table 3 Physicochemical properties of crude oil, neat and non-oxidative *Pongamia* and *Moringa* biodiesels

Property	Units	Equipment	Accuracy	ASTM D6751 B100		Crude oil		Neat biodiesels		Non-oxidative biodiesels		ASTM D975 diesel	Results
				Test method	Limits ^b	<i>Pongamia</i>	<i>Moringa</i>	<i>Pongamia</i>	<i>Moringa</i>	<i>Pongamia</i>	<i>Moringa</i>		
Kinematic viscosity at 40 °C	mm ² s ⁻¹	SVM 3000	0.1%	ASTM D445	1.9–6	44.17	33.26	5.13	4.43	6.50	4.33	1.3–4.1	3.85
Density at 15 °C	kg m ⁻³	SVM 3000	±0.1 kg m ⁻³	ASTM D1298	860–894	941.2	921.3	894.7	883.2	909.5	885.2	850	839.1
Oxidation stability	h	873 Rancimat	±0.01 h	EN ISO 14112	3 h min ^a	13.47	6.27	6.70	4.99	11.98	0.88	—	19.89
Calorific value	MJ kg ⁻¹	C2000 basic calorimeter	±0.001 MJ kg ⁻¹	ASTM D240	—	38.85	39.60	38.19	39.97	39.45	39.90	42–46	45.67
Cetane number	—	—	—	ASTM D613	47 min	—	—	56.13	45.97	56.60	49.28	40–55	48

^a Limit according to EN-14214. ^b Ref. 27 and 28. ^c Ref. 27.

3.4 Characterization of neat and non-oxidative biodiesels

The major physicochemical properties of neat and non-oxidative *Pongamia* and *Moringa* biodiesels are listed in Table 3 to compare with no. 2 diesel (B0). All the properties were compared with the ASTM D6751 standards. Cetane number was determined three times using fatty acid methyl ester composition with several empirical equations^{23–26} presented below:

$$\text{CN} = 46.3 + (5458/\text{SV}) - (0.225 \times \text{IV}) \quad (1)$$

$$\text{SV} = \sum (560 \times A_i) / M_{wi} \quad (2)$$

$$\text{IV} = \sum (254 \times A_i \times D) / M_{wi} \quad (3)$$

where A_i is the weight percentage of each fatty acid component, D is the number of double bonds in each fatty acid, M_{wi} is the molecular mass of each fatty acid component, SV is the saponification value and IV is the iodine value.

3.4.1 Kinematic viscosity. In Table 3, there is fluctuation in the change of the property for neat and non-oxidative biodiesels. The kinematic viscosity decreases for *Moringa* biodiesel from neat to non-oxidative, but increases for *Pongamia* biodiesel. However, both the biodiesels had higher viscosity than diesel for both neat and non-oxidative mode. Moreover, in case of crude oil, *Pongamia* had higher viscosity than *Moringa*. As viscosity influences the fuel injection system specially the spray atomization, penetration of the injected jet, air–fuel mixture combustion quality at low temperatures, it is very important for combustion quality. Biodiesels have higher viscosity than diesel fuel because of the presence of electronegative oxygen, which makes the biodiesels more polar than diesel.^{28–30} Hence, the reduction of oxygen from biodiesels can improve the viscosity.

3.4.2 Density. The changes in density are almost similar to the changes in kinematic viscosity except in the case of *Moringa* biodiesel, as shown in Table 3. The density increases for *Pongamia* and *Moringa* biodiesels from neat to non-oxidative mode. However, all the neat and non-oxidative biodiesels had a higher density than diesel. Among them, *Moringa* biodiesel had lower density range for both neat and non-oxidative mode. Crude *Pongamia* oil had higher density than *Moringa* similar as the neat and non-oxidative biodiesels. Density is an important parameter for fuel property as it affects the fuel atomization and combustion as well as other engine properties are also related to fuel density such as heating value, cetane number and viscosity. The density of biodiesel is normally higher than diesel as the density of biodiesel depends on its fatty acid composition, molar mass, water content and purity.^{28,29}

3.4.3 Oxidation stability. The oxidation stability increases for *Pongamia* biodiesel from neat to non-oxidative mode, whereas decreases for *Moringa* biodiesel from neat to non-oxidative mode, which was under the minimum requirement. This decrease indicates the lower oxidation stability of *Moringa* biodiesel from neat to non-oxidative mode. However, diesel had the highest oxidation stability among all crude oils, neat and non-oxidative biodiesels. Moreover, non-oxidative *Pongamia* biodiesel had higher oxidation stability after diesel among all other neat and non-oxidative biodiesels due to high monounsaturated fatty acid.

Oxidation stability affects the biodiesel quality by oxidizing it during storage for distribution or in the fuel system. Biodiesels are fatty acid methyl ester, which oxidize automatically to form aldehydes, ketones and resins and makes the fuel useless to run the engine. The oxidation rate of biodiesel depends on temperature, fatty acid composition, reaction catalyst, radiation intensity and light and it can be delayed by adding different antioxidants.^{28,29}

3.4.4 Calorific value. It can be inferred from the Table 3 that for *Moringa* biodiesel, the calorific value decreases from neat to non-oxidative mode but increases for *Pongamia* biodiesel. However, among all the biodiesels, *Moringa* had the highest calorific value for both neat and non-oxidative mode. Moreover, all the biodiesels and crude oils had lower calorific value than diesel. Biodiesels have lower heating value than diesel fuel because of the deviation in the hydrogen and carbon content and presence of high oxygen molecule that decreases the heating value by about 10–13% in biodiesel than diesel. Heating value of biodiesel increases with its number of carbon atoms and decreases with its number of double bonds.^{28,29} Therefore, it can be shown that in *Pongamia* biodiesel, the calorific value increases with increasing carbon molecules and decreasing oxygen molecules.

3.4.5 Cetane number. The cetane number for all biodiesels was increased from neat to non-oxidative mode, as seen in Table 3. However, *Pongamia* biodiesel had higher cetane number than *Moringa* for both neat and non-oxidative mode. Moreover, all the biodiesels had higher cetane number than diesel except neat *Moringa* and also non-oxidative *Moringa* had almost similar value as diesel. Cetane number is defined as the dimensionless measure of the ignition quality of diesel fuel during combustion of a compression ignition engine. It describes the fuel quality based on the ease of self-ignition of the particular fuel. Ignition delay (ID) period of diesel fuel is also indicated by it during the ignition period of injected diesel fuel in the combustion chamber. The higher ignition time lag indicates the lower cetane number and *vice versa*. The range of

cetane number in ASTM D6751 standards is based on the two experimental measured fuels named hexadecane ($C_{16}H_{34}$) with cetane number 100 and 2,2,4,4,6,8,8-heptamethylnonane with cetane number 15. The first one is an easily ignited fuel and the other one is highly resistive to ignite. Typically, biodiesels have higher cetane number than diesel fuel. 41–56 is the usual range of cetane number for no. 2 diesel and it should not be higher than 65.^{28,29} Therefore, in that case, *Moringa* biodiesel had the more suitable cetane number but as indicated earlier that lower polyunsaturated fatty acid indicates high cetane number and thus a low level of NO_x emissions, so non-oxidative *Pongamia* can perform better than *Moringa* biodiesel. Moreover, all the neat and non-oxidative *Pongamia* and *Moringa* biodiesels satisfied the requirements, which ensures the suitability of use of the biodiesels in the diesel engine without any modification by blending with diesel or in a pure form.

By analyzing all the properties, it can be observed that all the neat and non-oxidative *Pongamia* and *Moringa* biodiesels satisfied the requirements according to the ASTM D6751 standards, which ensure the suitability of use of those biodiesels in a diesel engine without any modification by blending with diesel or in a pure form.

3.5 Thermogravimetric analysis of neat and non-oxidative biodiesels

Thermogravimetric analysis of neat, non-oxidative biodiesels and diesel were conducted to understand the decomposition, thermal degradation behavior and volatility of those biodiesels.

In Fig. 3, the TGA curves of neat, non-oxidative *Pongamia*, *Moringa* biodiesels and diesel were compared. In this figure, all the curves had the similar trend. First, the TGA curves achieve ascending trend due to buoyancy and molecular adsorption effect but not in a distinct way and all of the neat and non-oxidative biodiesels and diesel were decomposed in only one step, which was clearly observed.² The decomposition temperature decreases from neat to non-oxidative biodiesels. Neat

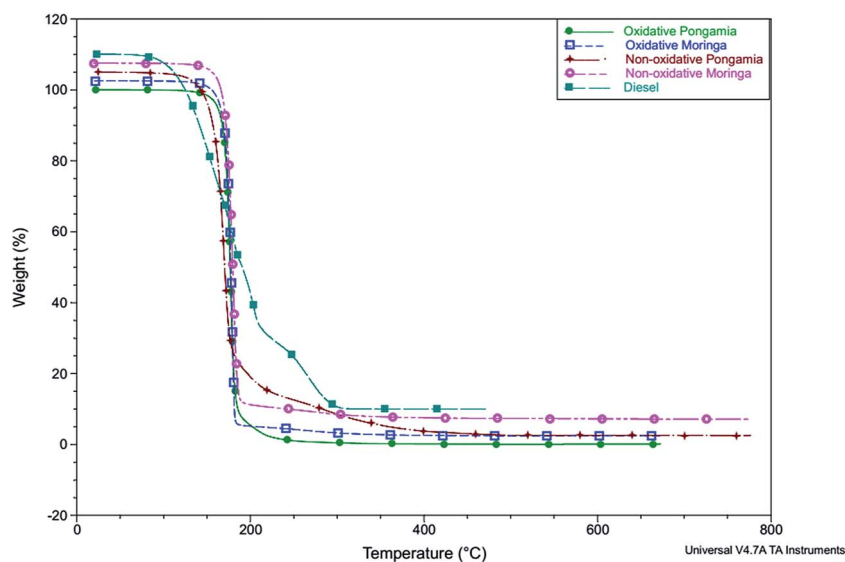


Fig. 3 TGA curves of neat, non-oxidative *Pongamia*, *Moringa* biodiesels and diesel at $50\text{ }^{\circ}\text{C min}^{-1}$ heating rate.

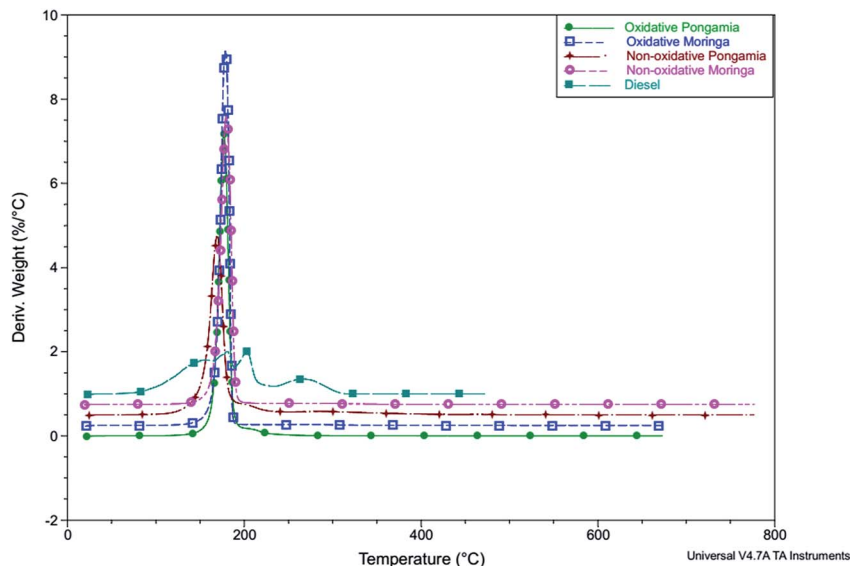


Fig. 4 DTG curves of neat, non-oxidative *Pongamia*, *Moringa* biodiesels and diesel at $50\text{ }^{\circ}\text{C min}^{-1}$ heating rate.

Pongamia and *Moringa* biodiesels had almost a similar thermal stability range. *Pongamia* and *Moringa* biodiesels were thermally stable up to $170.16\text{ }^{\circ}\text{C}$ and $172.20\text{ }^{\circ}\text{C}$, respectively. However, non-oxidative *Pongamia* and *Moringa* biodiesels were thermally stable up to $158.28\text{ }^{\circ}\text{C}$ and $171.78\text{ }^{\circ}\text{C}$, respectively. On the other hand, diesel was thermally stable up to $129.04\text{ }^{\circ}\text{C}$. Hence, *Moringa* biodiesel is thermally more stable than *Pongamia* biodiesel and diesel at both neat and non-oxidative mode. Then, with the increasing temperature, the TGA curves were descending due to volatilization of weak chemical bonds and small molecules. Around 99% weight loss took place at the temperature ranges from $95\text{ }^{\circ}\text{C}$ to $279\text{ }^{\circ}\text{C}$, $107\text{ }^{\circ}\text{C}$ to $317\text{ }^{\circ}\text{C}$ and $61\text{ }^{\circ}\text{C}$ to $302\text{ }^{\circ}\text{C}$ for neat *Pongamia*, *Moringa* biodiesels and diesel, respectively. On the other hand, for non-oxidative biodiesels, the 99% weight loss range increases compared to the neat biodiesels. Then, the final thermal degradation was observed with the 0.09%, 0.006% and 0.02024% carbon residue at the end of decomposition for neat *Pongamia*, *Moringa* biodiesels and diesel, respectively. However, in case of non-oxidative biodiesels, there were negative percentage of carbon residue observed at the end of the decomposition.^{2,31,32}

In Fig. 4, the derivative of thermogravimetric curves (DTG) are also presented. These curves showed the temperature at its peak point where the maximum rate of change of thermal decomposition (dm/dT_{max}) took place for all of the neat and non-oxidative biodiesels and diesel. From the figure, it can be seen that the peaks of the DTG curves occurred at $177\text{ }^{\circ}\text{C}$, $179\text{ }^{\circ}\text{C}$ and $203\text{ }^{\circ}\text{C}$ for neat *Pongamia*, *Moringa* biodiesels and diesel, respectively. For non-oxidative *Moringa* biodiesel, the peak was increased but it decreased for *Pongamia* biodiesel. Therefore, *Moringa* biodiesel had the highest temperature for the maximum rate of change of thermal decomposition (dm/dT_{max}) for both neat and non-oxidative mode, but lower than that of diesel.^{10,33}

From the two figures, it can be concluded that almost all the biodiesels and diesel had the similar TGA and DTG curves and thermal characteristics with slight variations. In Table 4, all the results are summarized.

3.6 DSC analysis of neat and non-oxidative biodiesels

Differential scanning calorimetry (DSC) is one of the measurement methods for determining the thermal stability of

Table 4 Thermal characteristics (TGA) of neat and non-oxidative *Pongamia*, *Moringa* biodiesels and diesel

Parameters	Neat biodiesels		Non-oxidative biodiesels		Diesel
	<i>Pongamia</i>	<i>Moringa</i>	<i>Pongamia</i>	<i>Moringa</i>	
Product weight (mg)	18.07	19.72	14.04	20.56	19.89
Decomposition temperature ($^{\circ}\text{C}$)	170.16	172.20	158.28	171.78	129.04
Volatility (%)	Not found	Not found	Not found	Not found	Not found
1 st weight loss (%mg per mg)	99.3	99.4	101.8	99.67	99.5
1 st weight loss temperature range ($^{\circ}\text{C}$)	95–279	107–317	57–444	95–353	61–302
Lost weight at 1 st weight loss (mg)	17.95	19.60	14.29	20.49	19.79
Residue (%mg per mg)	0.08	0.006	−2.48	−0.3379	0.02024
Weight at residue (mg)	0.0156	0.0013	−0.3481	−0.06946	0.004
Peak temperature ($^{\circ}\text{C}$)	177	179	169	180	203

biodiesels. It determines the differential heat flow of biodiesel samples either endothermic or exothermic in respect with a reference as a function of temperature. In other words, DSC measures the energy absorbed or released by a sample as it is heated or cooled.³⁴ In the DSC curves, heat flow (W g^{-1}) was plotted against temperature ($^{\circ}\text{C}$). In the curves, there were variations in transitions and in the inert nitrogen atmosphere, the transitions were endothermic, which means that the molecules of the samples were absorbing heat from surrounding. The melting point and the corresponding enthalpy for those temperatures can be determined from the heating curves and from the cooling curves crystallization point and corresponding enthalpy can be obtained. There was no glass transition found for all of the biodiesel samples.^{35–39}

In Fig. 5(a) and (b), DSC curves of neat *Pongamia* biodiesel for heating and cooling are shown, respectively. It represents all the parameters that are important to analysis the curves. The curves showed that there was no glass transition phase and only melting and freezing phases were visible. Therefore, it was clear from the curves that in heating curve, only endothermic and in cooling curve only exothermic reactions occurred. Moreover, the enthalpy change for melting and freezing was also presented in the curves, including the reaction temperature range and heat flow range.

In Fig. 6 and 7, the DSC curves for heating and cooling are presented for neat, non-oxidative *Pongamia*, *Moringa* biodiesels and diesel to compare their changes. For diesel and both neat and non-oxidative biodiesels, only cracking reactions occurred

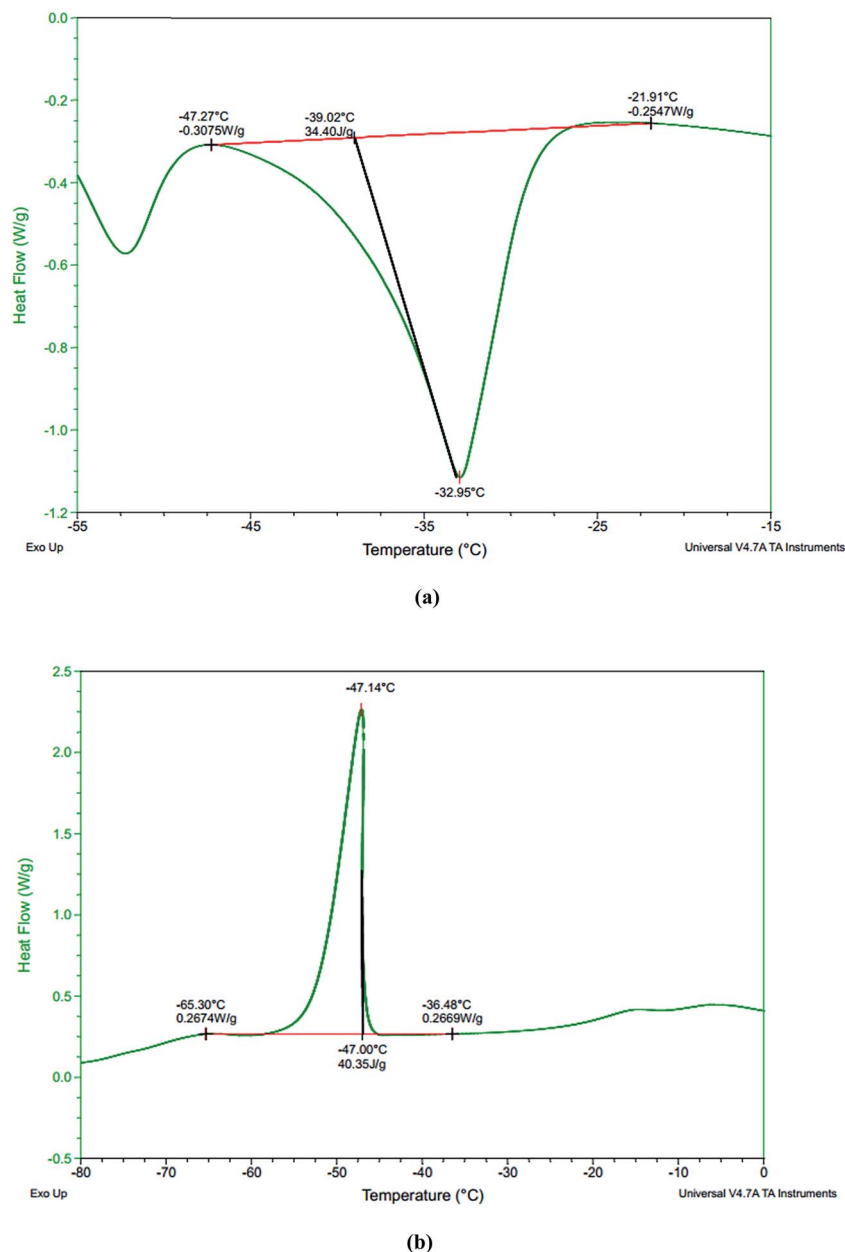


Fig. 5 DSC curve analysis of *Pongamia* biodiesel at $10^{\circ}\text{C min}^{-1}$ heating rate for (a) heating scans (b) cooling scans.

and there is no distillation region for both diesel and neat, non-oxidative biodiesels as per the figure. From the heating curves, the melting point of both neat and non-oxidative *Pongamia* was higher than both neat and non-oxidative *Moringa* biodiesels but lower than that of diesel. However, the melting point decreases for *Moringa* biodiesel from neat to non-oxidative mode but increases for *Pongamia* biodiesel. On the other hand, the enthalpy of melting decreases for all of the biodiesels from neat to non-oxidative mode. It was the highest for both neat and non-oxidative *Moringa* biodiesels and the lowest for diesel.

On the other hand, from the cooling curves, it is clearly comprehended that diesel had the highest and *Moringa* had the lowest crystallization temperature for both neat and non-oxidative mode, among all the biodiesels. However, the crystallization temperature decreases from neat to non-oxidative mode for both

Pongamia and *Moringa* biodiesels. Moreover, for the enthalpy of crystallization, it was highest for *Moringa* biodiesel for both neat and non-oxidative mode and lowest for diesel among all other biodiesels. In addition, the enthalpy of crystallization decreases for all of the biodiesels from neat to non-oxidative mode.

In Table 5, all the results for heating and cooling curves of DSC for diesel and neat, non-oxidative *Pongamia* and *Moringa* biodiesels are summarized to clearly understand the comparison among them.

3.7 Fourier transform infrared spectroscopy (FT-IR) analysis of neat and non-oxidative biodiesels

In this study, the FT-IR characteristics of all neat and non-oxidative biodiesels are presented to compare with diesel fuel

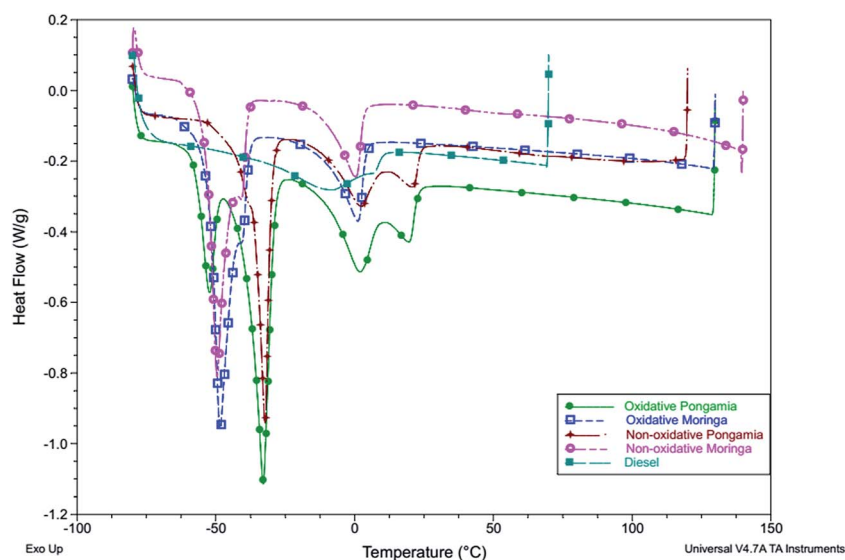


Fig. 6 DSC heating curves of neat, non-oxidative *Pongamia*, *Moringa* biodiesels and diesel at $10\text{ }^{\circ}\text{C min}^{-1}$.

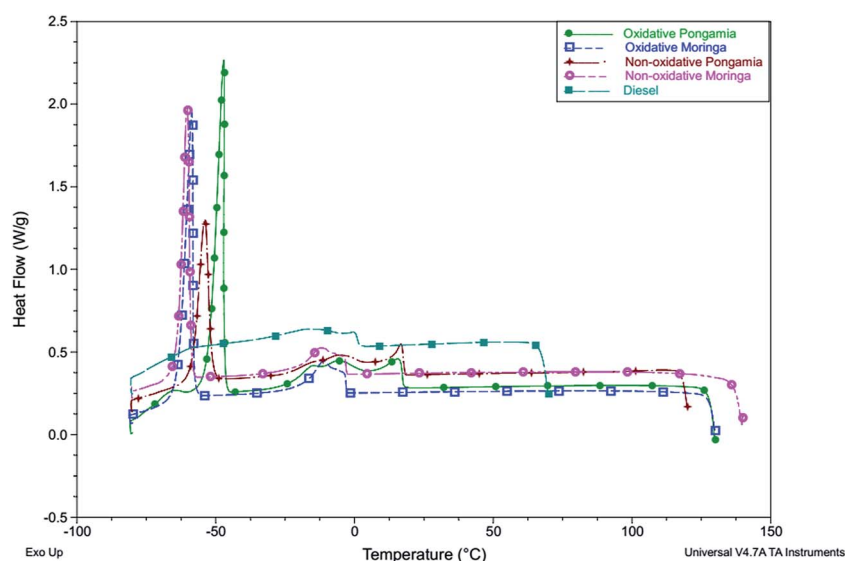


Fig. 7 DSC cooling curves of neat, non-oxidative *Pongamia*, *Moringa* biodiesels and diesel at $10\text{ }^{\circ}\text{C min}^{-1}$.

Table 5 Thermal characteristics (DSC) of neat and non-oxidative *Pongamia*, *Moringa* biodiesels and diesel

Parameter	Neat biodiesels		<i>Non-oxidative biodiesels</i>		Diesel
	<i>Pongamia</i>	<i>Moringa</i>	<i>Pongamia</i>	<i>Moringa</i>	
Product mass (mg)	17.7	14	11.2	5.8	15.8
Melting temperature (T_m) (°C)	−32.95	−48.49	−32.31	−49.52	−8.36
Onset temperature for melting (°C)	−39.02	−52.59	−36.84	−53.62	−39.03
Enthalpy of melting (ΔH) (J g ^{−1})	34.40	43.58	29.16	41.53	22.82
Temperature range of melting (°C)	−47.27 to −22.91	−70.81 to −33.34	−54.78 to −20.24	−70.90 to −25.62	−57.89 to −19.60
Heat flow range for melting (W g ^{−1})	−0.31 to −0.25	−0.09 to −0.16	−0.14 to −0.19	−0.04 to −0.11	−0.26–0.28
Crystallization temperature (T_c) (°C)	−47.14	−58.65	−53.97	−60.32	−16.49
Onset temperature for crystallization (°C)	−47.00	−58.24	−51.43	−59.02	1.67
Enthalpy of crystallization (ΔH) (J g ^{−1})	40.35	40.81	28.68	36.73	21.04
Temperature range of crystallization (°C)	−65.30 to −36.48	−74.33 to −46.69	−70.46 to −42.03	−73.02 to −48.12	−58.33–12.70
Heat flow range for crystallization (W g ^{−1})	0.2674–0.2669	0.09–0.18	0.13–0.22	0.11–0.16	0.28–0.29

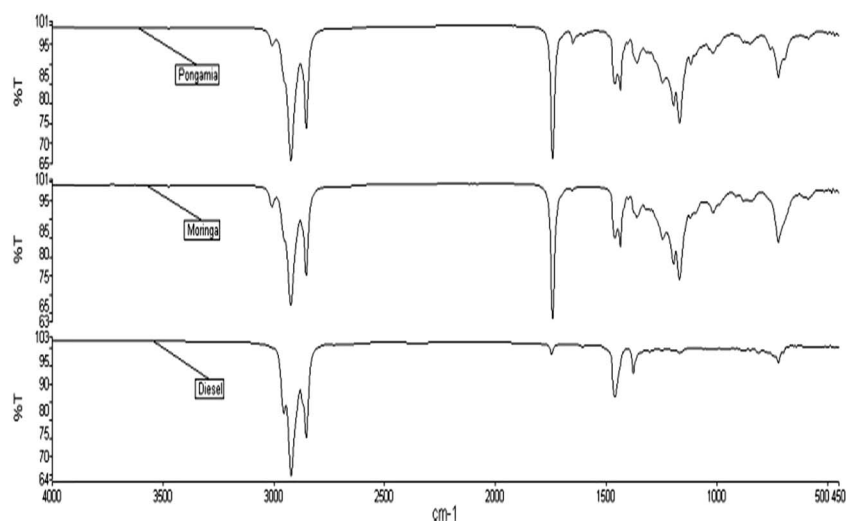
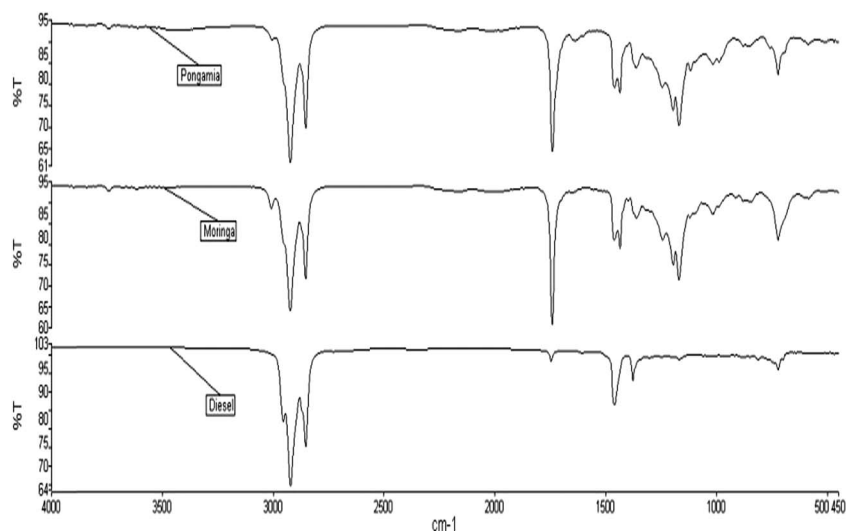
**Fig. 8** FT-IR spectrum of neat *Pongamia* and *Moringa* biodiesels compared with diesel.**Fig. 9** FT-IR spectrum of non-oxidative *Pongamia* and *Moringa* biodiesels compared with diesel.

Table 6 IR characteristics region for neat, non-oxidative biodiesels with diesel fuel

Frequency range (cm ⁻¹)	Bond type	Functional group	Neat biodiesels		Non-oxidative biodiesels		
			Pongamia	Moringa	Pongamia	Moringa	Diesel
2850–3000	C–H stretching	Alkanes	Present (2922.97 cm ⁻¹ , 65.92 %T); (2853.55 cm ⁻¹ , 74.08 %T)	Present (2923.49 cm ⁻¹ , 67.48 %T); (2853.98 cm ⁻¹ , 75.26 %T)	Present (2923.07 cm ⁻¹ , 61.90 %T); (2853.62 cm ⁻¹ , 69.8 %T)	Present (2923.56 cm ⁻¹ , 64.06 %T); (2854.07 cm ⁻¹ , 71.82 %T)	Present (2954.89 cm ⁻¹ , 81.75 %T); (2922.9 cm ⁻¹ , 64.65 %T); (2853.41 cm ⁻¹ , 75.18 %T)
1735–1750	C=O stretching	Esters	Present (1741.66 cm ⁻¹ , 66.58 %T)	Present (1741.53 cm ⁻¹ , 63.84 %T)	Present (1740.96 cm ⁻¹ , 64.33 %T)	Present (1741.66 cm ⁻¹ , 61.03 %T)	Absent
1350–1480	–C–H bending	Alkanes	Present (1462.97 cm ⁻¹ , 85.31 %T); (1435.92 cm ⁻¹ , 83.55 %T)	Present (1461.95 cm ⁻¹ , 85.47 %T); (1435.71 cm ⁻¹ , 83.09 %T)	Present (1436.12 cm ⁻¹ , 77.95 %T)	Present (1435.64 cm ⁻¹ , 79.04 %T)	Present (1462.24 cm ⁻¹ , 92.94 %T); (1377.22 cm ⁻¹ , 88.7 %T)
1000–1300	C–O stretching	Esters	Present (1195.72 cm ⁻¹ , 79.93 %T); (1168.30 cm ⁻¹ , 75.44 %T)	Present (1244.40 cm ⁻¹ , 84.92 %T); (1195.63 cm ⁻¹ , 78.25 %T); (1169.46 cm ⁻¹ , 74.28 %T); (1120.07 cm ⁻¹ , 90.71 %T)	Present (1169.09 cm ⁻¹ , 70.48 %T)	Present (1169.62 cm ⁻¹ , 71.69 %T)	Absent
700–725	C–H rock	Alkanes	Absent	Present (722.52 cm ⁻¹ , 84.14 %T)	Present (722.82 cm ⁻¹ , 82.33 %T)	Present (722.64 cm ⁻¹ , 81.10 %T)	Present (722.04 cm ⁻¹ , 95.87 %T)
2500–3300	O–H stretching	Carboxylic acids	Absent	Absent	Absent	Absent	Absent

and also to confirm that the functional groups presented in non-oxidative biodiesels were similar to neat biodiesels and diesel. This proves the suitability of those biodiesels in the diesel engine without any modification.

In Fig. 8 and 9, the IR spectrum of neat and non-oxidative *Pongamia* and *Moringa* biodiesels are shown in comparison to diesel fuel. Table 6 summarized all the frequency range, functional groups, absorbance peaks and percent transmittance (%T) for all neat and non-oxidative biodiesels along with diesel fuel. There is slight difference in the functional group present between neat and non-oxidative biodiesels. All the neat and non-oxidative biodiesels contained esters and the absence of any broad peaks of O–H stretching vibration of carboxylic acids in the region of 2500–3300 cm⁻¹ indicates the absence of moisture in the biodiesels and diesel. Moreover, the %T decreases from neat to non-oxidative mode for all biodiesels.^{19,31,40}

All the non-oxidative biodiesels satisfied the minimum requirements and had some improvements in their properties with very few exceptions to be used as an alternative fuel mixed with diesel instead of neat biodiesels. This new form of biodiesels will affect the performance of engine by reducing the NO_x emissions as well as maintain the other performance and exhaust emissions similar to neat biodiesels. However, the non-oxidative biodiesels is an alternative fuel source of the future for commercial use in large scale.

4. Conclusions

In this study, non-oxidative biodiesels were characterized by fuel physicochemical property, FAME composition, thermogravimetric and IR analysis and were compared with neat biodiesels and diesel fuel to determine the suitability of the biodiesels to be used in the diesel engine according to stability and quality. By considering and optimizing all the properties, it can be said that non-oxidative *Pongamia* has high suitability to be used in a diesel engine, although it has higher viscosity and density than its neat biodiesel; moreover, it had an improved oxidation stability and calorific value. Further research can be carried out to further improve those properties. The findings of this study are summarized here:

- The oxidation of iron bars was higher for *Pongamia* biodiesel than for *Moringa* biodiesel.
- The oxygen reduction percentage was higher for *Pongamia* than for *Moringa* biodiesel.
- The kinematic viscosity of *Moringa* biodiesel was decreased due to reduction of oxygen content but it increases for *Pongamia* biodiesel. Density increases for both *Pongamia* and *Moringa* biodiesels for the reduction of oxygen content.
- Non-oxidative *Pongamia* had the highest oxidation stability after diesel among other biodiesels.
- *Pongamia* biodiesel had increased calorific value due to the reduction of oxygen.
- Non-oxidative *Pongamia* had the highest cetane number among other neat and non-oxidative biodiesels and diesel. Lower polyunsaturated fatty acid indicates high cetane number and thus low level of NO_x emissions. Hence, non-oxidative *Pongamia* can reduce more NO_x compared to *Moringa* biodiesel.

• TGA and DSC analysis confirmed the thermal, oxidation and storage stability for both the non-oxidative biodiesels compared with neat biodiesels and diesel. For all biodiesels and diesel, no volatile characteristics were found.

• FT-IR analysis confirmed the suitability of all non-oxidative biodiesels to be used with diesel fuel replacing the neat biodiesels by defining the esters content and transmittance rate of those biodiesels.

Acknowledgements

The authors would like to acknowledge the University of Malaya for financial support through High Impact Research grant UM.C/HIR/MOHE/ENG/07. Thanks to Mr Solaiman and Mr Ismail for their help in oxygen reduction process and thermogravimetric analysis test, respectively.

References

- 1 T. Vega-Lizama, L. Díaz-Ballote, E. Hernández-Mézquita, F. May-Crespo, P. Castro-Borges, A. Castillo-Atoche, G. González-García and L. Maldonado, *Fuel*, 2015, **156**, 158–162.
- 2 H. Li, S.-l. Niu, C.-m. Lu and S.-q. Cheng, *Energy Convers. Manage.*, 2015, **98**, 81–88.
- 3 M. M. Conceição, V. J. Fernandes, A. S. Araújo, M. F. Farias, I. M. Santos and A. G. Souza, *Energy Fuels*, 2007, **21**, 1522–1527.
- 4 J. Gardya, A. Hassanpoura, X. Laia, A. Cunliffeb and M. Rehana, in *International Conference on Environment and Renewable Energy (ICERE)*, At Cité Internationale Universitaire de Paris, 17 Boulevard Jourdan, Paris, France, 2014.
- 5 S. Jain and M. Sharma, *Renewable Sustainable Energy Rev.*, 2011, **15**, 438–448.
- 6 G. Çaylı and S. Küsefoğlu, *Fuel Process. Technol.*, 2008, **89**, 118–122.
- 7 Y. Lai, B. Wang, X. Chen, Y. Yuan, L. Zhong, X. Qiao, Y. Zhang, M. Yuan, J. Shu and P. Wang, *Biotechnology*, 2015, **14**, 9–15.
- 8 S. M. A. Rahman, H. H. Masjuki, M. A. Kalam, M. J. Abedin, A. Sanjid and H. Sajjad, *Energy Convers. Manage.*, 2013, **76**, 362–367.
- 9 P. Varanasi, B. Knierim, E. Bosneaga, L. Sun, M. Auer, P. Sarkar and S. Singh, *Quantifying Bio-Engineering: The Importance of Biophysics in Biofuel Research*, INTECH Open Access Publisher, 2011.
- 10 P. Chand, V. Reddy, J. G. Verkade, T. Wang and D. A. Grewell, in *Agricultural and Biosystems Engineering Conference Papers, Posters and Presentations*, 2008.
- 11 S. Jain and M. Sharma, *Fuel*, 2012, **93**, 252–257.
- 12 M. Salahelddeen, M. Aroua, A. Mariod, S. F. Cheng and M. A. Abdelrahman, *Ind. Crops Prod.*, 2014, **61**, 49–61.
- 13 B. R. Moser, *Fuel*, 2012, **92**, 231–238.
- 14 A. Karmakar, S. Karmakar and S. Mukherjee, *Bioresour. Technol.*, 2010, **101**, 7201–7210.
- 15 S. L. Nettles-Anderson and D. B. Olsen, *Survey of straight vegetable oil composition impact on combustion properties 0148-7191*, *SAE Technical Paper*, 2009.
- 16 A. E. Atabani, M. Mofijur, H. H. Masjuki, I. A. Badruddin, M. A. Kalam and W. T. Chong, *Ind. Crops Prod.*, 2014, **60**, 130–137.
- 17 U. Rashid, F. Anwar, B. R. Moser and G. Knothe, *Bioresour. Technol.*, 2008, **99**, 8175–8179.
- 18 M. Mofijur, H. H. Masjuki, M. A. Kalam, A. E. Atabani, M. I. Arbab, S. F. Cheng and S. W. Gouk, *Energy Convers. Manage.*, 2014, **82**, 169–176.
- 19 M. N. Nabi, S. M. N. Hoque and M. S. Akhter, *Fuel Process. Technol.*, 2009, **90**, 1080–1086.
- 20 M. Naik, L. C. Meher, S. N. Naik and L. M. Das, *Biomass Bioenergy*, 2008, **32**, 354–357.
- 21 P. T. Scott, L. Pregelj, N. Chen, J. S. Hadler, M. A. Djordjevic and P. M. Gresshoff, *BioEnergy Res.*, 2008, **1**, 2–11.
- 22 N. Mukta and Y. Sreevalli, *Ind. Crops Prod.*, 2010, **31**, 1–12.
- 23 M. M. Rahman, M. H. Hassan, M. A. Kalam, A. E. Atabani, L. A. Memon and S. A. Rahman, *J. Cleaner Prod.*, 2014, **65**, 304–310.
- 24 S. M. A. Rahman, H. H. Masjuki, M. A. Kalam, M. J. Abedin, A. Sanjid and M. M. Rahman, *Renewable Energy*, 2014, **68**, 644–650.
- 25 K. Krisnangkura, *J. Am. Oil Chem. Soc.*, 1986, **63**, 552–553.
- 26 P. Devan and N. Mahalakshmi, *Fuel Process. Technol.*, 2009, **90**, 513–519.
- 27 A. E. Atabani, A. S. Silitonga, I. A. Badruddin, T. M. I. Mahlia, H. H. Masjuki and S. Mekhilef, *Renewable Sustainable Energy Rev.*, 2012, **16**, 2070–2093.
- 28 A. E. Atabani, A. S. Silitonga, H. C. Ong, T. M. I. Mahlia, H. H. Masjuki, I. A. Badruddin and H. Fayaz, *Renewable Sustainable Energy Rev.*, 2013, **18**, 211–245.
- 29 I. Barabás and I.-A. Todoruț, in *Biodiesel-Quality, Emissions and By-Products*, 2011, pp. 3–28.
- 30 T. M. Y. Khan, A. E. Atabani, I. A. Badruddin, A. Badarudin, M. S. Khayoon and S. Triwahyono, *Renewable Sustainable Energy Rev.*, 2014, **37**, 840–851.
- 31 M. Farooq, A. Ramli and D. Subbarao, *J. Cleaner Prod.*, 2013, **59**, 131–140.
- 32 C. S. Madankar, A. K. Dalai and S. N. Naik, *Ind. Crops Prod.*, 2013, **44**, 139–144.
- 33 H. Kandala, Masters thesis, 2009, 93.
- 34 J. Leifeld, *Org. Geochem.*, 2007, **38**, 112–127.
- 35 R. O. Dunn, *J. Am. Oil Chem. Soc.*, 1999, **76**, 109–115.
- 36 G. Knothe and R. O. Dunn, *J. Am. Oil Chem. Soc.*, 2009, **86**, 843–856.
- 37 E. Topa, MS thesis, Middle East Technical University, Turkey, 2010.
- 38 S. Jain and M. Sharma, *Renewable Sustainable Energy Rev.*, 2010, **14**, 1937–1947.
- 39 M. M. Conceição, R. A. Candeia, F. C. Silva, A. F. Bezerra, V. J. Fernandes and A. G. Souza, *Renewable Sustainable Energy Rev.*, 2007, **11**, 964–975.
- 40 M. Ndana, J. Grace, F. Baba and U. Mohammed, *International Journal of Science, Environment and Technology*, 2013, **2**, 1116–1121.